Erratum

Ontogenetic changes in jaw-muscle architecture facilitate durophagy in the turtle *Sternotherus minor*

J. B. Pfaller, P. M. Gignac and G. M. Erickson

10.1242/jeb059493

There was an error published in the original online version of *J. Exp. Biol.* **214**, 1655-1667. This error occurred in both the PDF and full-text versions of the online article. The print version is correct.

The accepted date was incorrectly given as 21 December 2011. The correct accepted date is 21 December 2010.

We apologise sincerely to authors and readers for any inconvenience this error may have caused.

The Journal of Experimental Biology 214, 1655-1667

doi:10.1242/jeb.048090

RESEARCH ARTICLE

Ontogenetic changes in jaw-muscle architecture facilitate durophagy in the turtle *Sternotherus minor*

Joseph B. Pfaller*, Paul M. Gignac and Gregory M. Erickson

Department of Biological Science, Florida State University, Tallahassee, FL 32306, USA

*Author for correspondence at present address: University of Florida, Gainesville, FL 32611, USA (jpfaller@ufl.edu)

Accepted 21 December 2011

SUMMARY

Differential scaling of musculoskeletal traits leads to differences in performance across ontogeny and ultimately determines patterns of resource use during development. Because musculoskeletal growth of the feeding system facilitates high bite-force generation necessary to overcome the physical constraints of consuming more durable prey, durophagous taxa are well suited for investigations of the scaling relationships between musculoskeletal growth, bite-force generation and dietary ontogeny. To elucidate which biomechanical factors are responsible for allometric changes in bite force and durophagy, we developed and experimentally tested a static model of bite-force generation throughout development in the durophagous turtle *Sternotherus minor*. Moreover, we quantified the fracture properties of snails found in the diet to evaluate the relationship between bite force and the forces required to process durable prey. We found that (1) the static bite-force model accurately predicts the ontogenetic scaling of bite forces, (2) bite-force positive allometry is accomplished by augmenting muscle size and muscle pennation, and (3) the rupture forces of snails found in the diet show a similar scaling pattern to bite force across ontogeny. These results indicate the importance of muscle pennation for generating high bite forces while maintaining muscle size and provide empirical evidence that the allometric patterns of musculoskeletal growth in *S. minor* are strongly linked to the structural properties of their primary prey.

Key words: bite force, feeding, biomechanics, turtles, pennation, muscle architecture.

INTRODUCTION

Understanding how scaling of musculoskeletal traits leads to differences in performance across ontogeny is a cardinal goal of both functional morphology and biomechanics (Schmidt-Nielson, 1984; Emerson and Bramble, 1993). Maximum bite-force generation and the functional consequences of scaling in cranial morphology are particularly important for vertebrates that process and consume robust food resources (e.g. bone, mollusks, seeds), a foraging mode known as durophagy. Durophagy is associated with allometric changes in cranial morphology and bite force that allow consumers to expand their diet (Erickson et al., 2003) or specialize on prey for which there is little or no competition (Wainwright, 1987; Bulté et al., 2008). Taxa showing positively allometric patterns of musculoskeletal growth and performance may gain a competitive advantage over those with isometric development patterns by obtaining access to more diverse or exclusive food resources earlier in life (Kolmann and Huber, 2009). Previous studies have also shown that individuals with higher bite forces require less time to consume certain prey items (Herrel et al., 2001; Verwaijen et al., 2002; Van der Meij and Bout, 2006). This suggests that an additional benefit of developing allometrically greater bite forces is that durophagous taxa can increase the net rate of energy intake when foraging (optimal foraging) (MacArthur and Pianka, 1966), and presumably enhance their fitness (Anderson et al., 2008). Because the implications for growth patterns that facilitate high bite-force generation are apparent (Kolmann and Huber, 2009), the feeding systems of durophagous taxa are well suited for investigations of the scaling relationships between musculoskeletal growth, feeding performance and dietary ontogeny.

An ontogenetic (or phylogenetic) increase in maximum bite force can be achieved in several ways (Herrel et al., 2002). Firstly, it can be afforded through increased body size as greater muscle volume confers absolutely greater force generation (Schmidt-Nielson, 1984; Anderson et al., 2008). Secondly, ontogenetic increases in the jaw-closing musculature (invariably associated with increased head dimensions), without changes in muscle physiology, lever mechanics or body size, will also lead to absolute increases in bite force. Thirdly, biomechanical theory predicts that bite-force generation may additionally be increased by augmenting the mechanical advantage of the system or by increasing muscle-force generation, or through a combination of the two (Cochran, 1982). Mechanical advantage (equivalent to the in-lever:out-lever ratio only for an ideal frictionless mechanism) can be enhanced by shifting muscle insertion points and angles or repositioning the bite point (behaviorally or through growth), or both. Muscle-force generation is a function of the physiological cross-sectional area (PCSA) of the active muscles (Emerson and Bramble, 1993), and can be increased by augmenting the relative mass of the muscle or changing the fiber architecture (i.e. the degree and angle of pennation) (Gans and De Vree, 1987), or both. All available data from a broad range of durophagous taxa show that bite forces increase disproportionately relative to changes in head and body dimensions across ontogeny (i.e. positive allometry) (Herrel and Gibb, 2006; Anderson et al., 2008). These results suggest that the scaling of traits related to musculoskeletal biomechanics is most likely to explain the allometric patterns of bite force among durophagous taxa (Herrel et al., 2002; Herrel and O'Reilly, 2006). Differential scaling of these parameters has been hypothesized to explain bite-force positive allometry. However, with the exception

of fishes (Wainwright, 1987; Hernández and Motta, 1997; Huber and Motta, 2004; Grubich, 2005; Herrel et al., 2005; Huber et al., 2006; Huber et al., 2008; Kolmann and Huber, 2009), few studies have quantified the musculoskeletal biomechanics of ontogenetic series to support these assertions. As a result, it is not clear which patterns of musculoskeletal scaling associated with bite-force positive allometry are prevalent among tetrapods.

The vertebrate cranium is characterized by anatomical integration and complexity, in which traits, such as kinetic joints, dentition and jaw mobility, collectively interact to affect feeding performance parameters (e.g. bite force or jaw kinematics). Thus, attempts to model the biomechanics of vertebrate feeding behaviors typically apply simplifying assumptions, which limit the efficacy of these models to address particular ecological and evolutionary questions. Conversely, the feeding apparatus of turtles (Chelonia) requires fewer simplifying assumptions because it is edentulous and akinetic, and jaw movements are mostly orthogonal. Thus, turtle feeding systems are suitable for biomechanical modeling and provide an enhanced utility for investigating scaling relationships in a tetrapod vertebrate. While considerable attention has been given to the organization of cranial elements and musculature in turtles (Schumacher, 1973), no studies have investigated how bite-force generation relates to musculoskeletal growth and dietary ontogeny. Herein, we examine the relationship between musculoskeletal feeding biomechanics, bite-force generation and diet in an ontogenetic series of loggerhead musk turtles, *Sternotherus minor* (Agassiz 1857). Adults of this species develop hypertrophied skulls and jaw musculature, as well as expanded triturating surfaces (Pfaller et al., 2010), which allow for increased durophagy as animals grow (Zappalorti and Iverson, 2006). Juveniles have a generalist diet, while adults primarily consume snails and clams (Tinkle, 1958). In addition, bite force in *S. minor* has been shown to increase with positive allometry relative to external morphological features (Pfaller et al., 2010). This suggests either consequent allometric changes to the musculoskeletal biomechanics of the feeding apparatus across ontogeny or substantial behavioral changes in biting motivation. In the present study, we first derived maximum bite-force estimates throughout development based on a static model of the jaw adductor system that incorporates muscle pennation and assumes maximum motivation, and compared these to bite-force measurements recorded from the same individuals. Second, we determined the scaling relationships among biomechanical variables and between those variables and bite force, to elucidate which of these factors are responsible for the allometric patterns of force production. Finally, we quantified the rupture properties of the primary prey item of adult *S. minor*, *Goniobasis* (Lea 1862) snails, to evaluate the ontogenetic relationship between bite-force generation and the forces required to orally process durable prey found in the diet.

MATERIALS AND METHODS

Experimental animals

On 26 April 2008, an ontogenetic series composed of 30 *S. minor* [yearlings (26 g, *ca*. 53.2 mm carapace length) to adults (331 g, *ca*. 126.5 mm carapace length)] were hand captured in the Rainbow River, Marion County, FL, USA (Florida Fish and Wildlife Conservation Commission permit WX06362a). Upon capture, all individuals were numbered and subaerial bite-force generation was measured (see below). The specimens were subsequently killed through intravenous overdoses of pentobarbital sodium (390 mg ml^{-1}; 0.5 ml per individual) and dissected for quantification of cranial musculoskeletal anatomy, biomechanical modeling of bite-force generation, and dietary analyses. Experiments were conducted according to Florida State University Animal Care and Use Committee guidelines (protocol no. 0011).

Observed bite-force generation

To measure bite force from live individuals, we used the protocol and apparatus described previously (Pfaller et al., 2010). The apparatus was composed of a Type 9212 high impedance load cell (Kistler Instrument Corp., Amherst, NY, USA) sandwiched between two stainless-steel cantilever beams, such that the voltage output routed through a charge amplifier (Type 5995A, Kistler Instrument Corp.) was linearly proportional to the compressive forces applied to the beams. Two bite-plate configurations were used depending on the size of turtle being tested: a 3 mm gape configuration for turtles ≤100 g and a 5 mm gape configuration for turtles >100 g. Leather strips were affixed to the biting surface of each beam to prevent injury to the rhamphotheci and ensure an invariant bite point on the apparatus (Erickson et al., 2003). The specimens were manually restrained, and the cantilever beams were placed unilaterally between the jaws, centered mesiodistally at the trough of the crushing surface along the lower beak. This location represents the site along the jaw at which *S. minor* processes snails (Pfaller, 2009). Contact invariably elicited an aggressive bite in turtles of all sizes. Three bite-force trials at 2 min intervals were made for each specimen. The highest value for each specimen was used in *post hoc* analyses to represent maximum bite-force capacity.

Static bite-force model

A static model of bite-force generation was derived by estimating the forces produced by the entire suite of muscles that function to adduct the jaws in *S. minor*. These include the Musculus adductor mandibulae complex: M. add. mand. externus, M. add. mand. posterior and M. add. mand. internus (Fig. 1). We followed the identification, attachment points and nomenclature for these muscles used by Schumacher (Schumacher, 1973). Specifically, the M. add. mand. externus is the largest jaw adductor in turtles and is composed of the Pars profunda, Pars superficialis and Pars media. In the upper temporal fossa, the Pars profunda and Pars superficialis have a pennate arrangement with fibers inserting around the centrally located external tendon: the Pars superficialis laterally and the Pars profunda medially. The attachment area for the Pars profunda is enlarged by a secondary lobe of the external tendon that runs dorsally and an additional tendon that runs anteriorly from the back of the skull. Because of this tendonous arrangement, the Pars profunda is composed of three muscle subdivisions: α, β, γ (Fig. 1A,B). The external tendon runs anteroventrally to the trochlear process where it reflects ventrally *via* the trochlear cartilage toward a broad base on the lower jaw. The Pars media is not attached to the external tendon and its fibers are located entirely within the lower temporal fossa (Fig. 1B). The M. add. mand. posterior is a small, parallel-fibered muscle also located entirely within the lower temporal fossa (Fig. 1C). The M. add. mand. internus lines the medial wall of the lower temporal fossa and is subdivided into the M. pseudotemporalis and M. pterygoideus, which both converge on the internal tendon and attach to the medial side of the lower jaw near the jaw joint (Fig. 1C). In the present study, we considered all eight muscle subdivisions that collectively function to adduct the jaws: Pars superficialis and Pars profunda α, β, γ (both attached to the external tendon), Pars media, M. posterior, M. pseudotemporalis and M. pterygoideus.

For each of the 30 specimens, all eight jaw adductor subdivisions were excised from the right side of the head, photographed separately and immediately weighed to the nearest thousandth of a gram using a digital scale (model AR-1530, Ohaus Corp., Pine

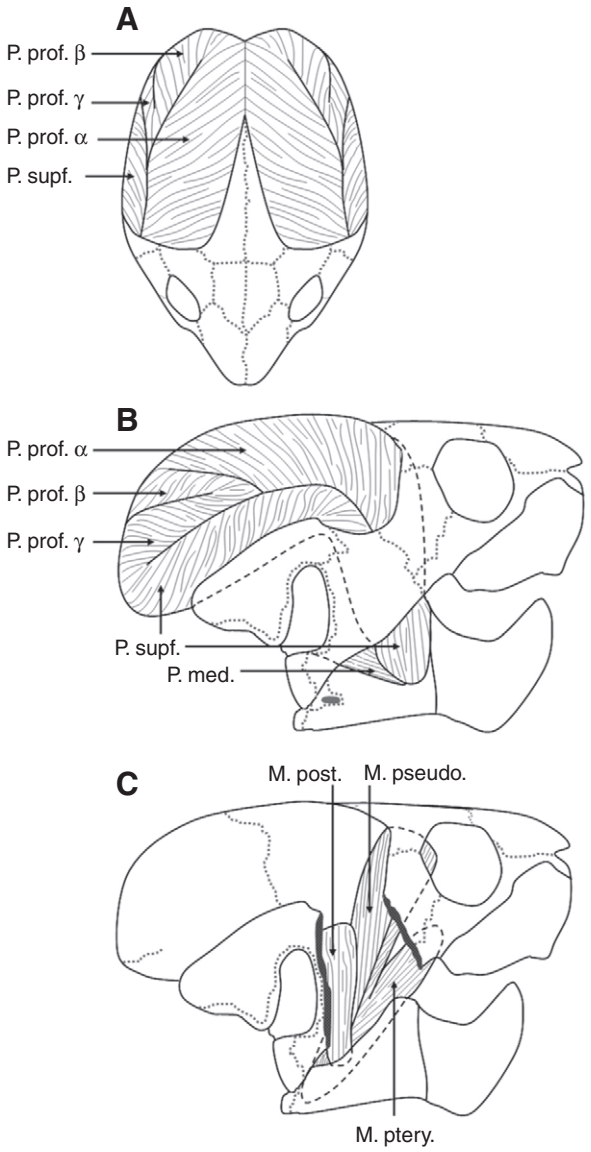

Fig. 1. Jaw adductor musculature of *Sternotherus minor*. (A) Dorsal and (B) lateral view of the Musculus adductor mandibulae externus (P. prof., Pars profunda; P. supf., Pars superficialis; P. med., Pars media); (C) lateral view of the Musculus adductor mandibulae posterior (M. post.) and internus (M. pseudo., M. pseudotemporalis; M. ptery., M. pterygoideus).

Brook, NJ, USA). Digital photographs were taken perpendicular to the head throughout each dissection from both lateral and dorsal views (model D40, Nikon Corp., Tokyo, Japan), and were used to develop the three-dimensional coordinate system of the static bite-force model (see below). For each subdivision, muscle-fiber lengths were measured from 10 locations selected throughout each muscle body. The pennation angles of the fibers attached to the external tendon (Pars superficialis and Pars profunda α, β, γ) were measured from 10 locations selected throughout each muscle body using the aforementioned digital photographs (ImageJ v. 1.40, National Institutes of Health, Bethesda, MD, USA). [Note: during the dissections we found that pennation in the M. add. mand. internus (M. pseudotemporalis and M. pterygoideus) is weakly developed (angles <5 deg). Therefore, pennation in these subdivisions was not considered in the theoretical bite-force estimates.]

Using these data, the mean PCSA (cm^2) of each muscle subdivision was computed as muscle mass (g) divided by mean fiber length (cm) and muscle density ($g\,cm^{-3}$). Muscle density was assumed to be $1\,g\,cm^{-3}$ (Powell et al., 1984):

$$\mathrm{PCSA} = \frac{\text{muscle mass}}{\text{muscle density}} \times \frac{1}{\text{fiber length}} \times \cos\theta \ . \quad (1)$$

The mean PCSA of the Pars superficialis and the three bodies of the Pars profunda (α, β, γ) includes a term representing the cosine of the mean pennation angle (θ) for each muscle subdivision (Powell et al., 1984). To estimate muscle force (**F**, in N) for each muscle subdivision, PCSA was multiplied by a muscle stress value of $25\,N\,cm^{-2}$. Empirically derived muscle stress values for chelonian cranial muscles are not available and $25\,N\,cm^{-2}$ is commonly used by investigators attempting to determine theoretical whole muscle-force generation in vertebrates (e.g. Cleuren et al., 1995; Herrel et al., 1999; Herrel et al., 2008). Other verified muscle-stress values (20 and $30\,N\,cm^{-2}$) were tested in an earlier study (Pfaller, 2009).

Bite-force generation was then estimated by developing a static equilibrium model of the forces generated by the jaw adductor muscles and the lever mechanics of the feeding system (Cleuren et al., 1995; Herrel et al., 2008; Huber et al., 2005; Huber et al., 2008). Photographs taken laterally and dorsally during muscle dissections were used to develop three-dimensional coordinate systems for each individual. Using the anterodorsal tip of the premaxilla as the origin, the distances to the muscle attachment points of all muscles and the positions of the jaw joint and bite point were measured (Fig. 2). For all individuals, the orientation of muscles was determined for a gape angle of approximately 10 deg, which represents a nearly closed gape similar to that for the bite-force trials and when prey items are being crushed (Cleuren et al., 1995; Pfaller, 2009). Force vectors were determined for each muscle based on theoretical muscle force and three-dimensional coordinates of the origin and insertion (Davis et al., 2010). Because of the strictly orthogonal jaw movements in this system bite forces are realized in the sagittal plane only; therefore, the medially directed component of each muscle force vector was removed to account for the three-dimensional orientation of the adductor muscles. Additionally, in-lever lengths (IL) for each muscle were measured as the perpendicular distance from the three-dimensional coordinates of the jaw joint to the muscle-force vector (Fig. 2B–E). The Pars superficialis and Pars profunda (α, β, γ) attach to the external tendon and act along the same IL (Fig. 2A,B). Resolved in-lever length (RIL) was estimated for each specimen by calculating a weighted mean of the in-levers based on their respective muscle forces (Huber et al., 2006). The out-lever length (OL) for biting at the trough of the crushing surfaces along the lower jaw (directly lateral to the mid-jaw symphysis; Fig. 2) is the same for all muscles within a given specimen and was determined from the three-dimensional coordinates of the bite point and the jaw joint. Because we are assuming an ideal (frictionless) mechanism, mechanical advantage (MA) was computed as RIL divided by OL.

For a jaw system in static equilibrium, the rotational forces generated by the muscular forces acting about the jaw joint must balance the force of biting (Cochran, 1982; Ellis et al., 2008). Right-side bite-force generation (RBF), therefore, was estimated by Eqn 2:

$$\mathrm{RBF} = \frac{(\mathbf{F}_{\mathrm{sup,pro}} \times \mathrm{IL}_{\mathrm{sup,pro}})}{\mathrm{OL}} + \frac{(\mathbf{F}_{\mathrm{med}} \times \mathrm{IL}_{\mathrm{med}})}{\mathrm{OL}} + \frac{(\mathbf{F}_{\mathrm{post}} \times \mathrm{IL}_{\mathrm{post}})}{\mathrm{OL}} + \frac{(\mathbf{F}_{\mathrm{pseudo,ptery}} \times \mathrm{IL}_{\mathrm{pseudo,ptery}})}{\mathrm{OL}} \ , \quad (2)$$

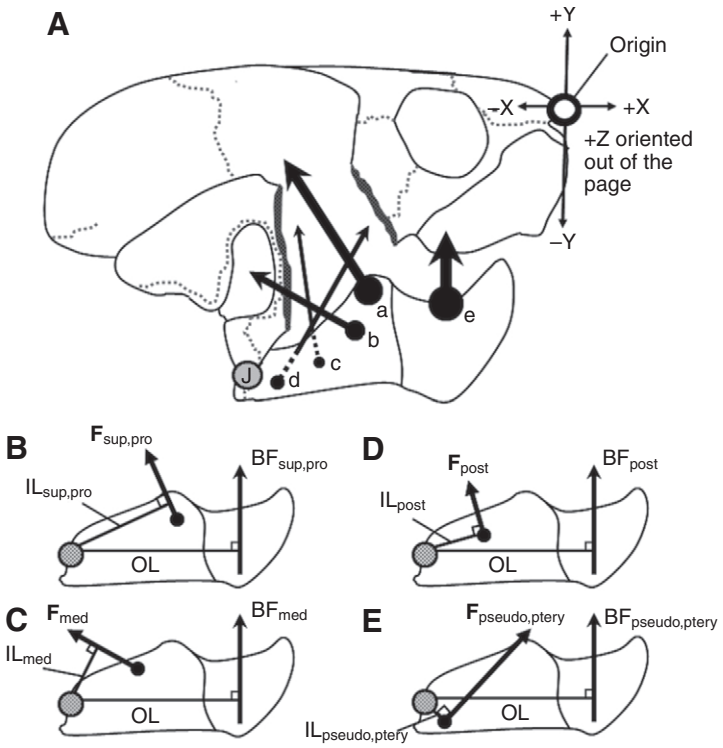

Fig. 2. Schematic diagram of the skull and jaw of *S. minor*. (A) Three-dimensional coordinate system used for vector analysis, and the two-dimensional origins and directions of forces acting on the lower jaw relative to the skull. a, Pars superficialis, profunda complex; b, Pars media; c, M. posterior; d, M. pseudotemporalis, pterygoideus complex; e, bite force; J, jaw joint. (B–E) Free-body diagrams of the lower jaw indicating force directions and lever lengths for jaw adductor musculature and bite force. F, muscle force; BF, bite force; IL, in-lever length; OL, out-lever length; J, jaw joint (shaded circle). (B) Pars superficialis, profunda complex, (C) Pars media, (D) M. posterior, and (E) M. pseudotemporalis, pterygoideus complex.

where $\mathbf{F}_{sup,pro}$ and $IL_{sup,pro}$ are the muscle force and in-lever length, respectively, for the Pars superficialis and Pars profunda collectively (Fig. 2B); $\mathbf{F}_{med}$ and IL_{med} are the muscle force and in-lever length, respectively, for the Pars media (Fig. 2C); $\mathbf{F}_{post}$ and IL_{post} are the muscle force and in-lever length, respectively, for the M. posterior (Fig. 2D); $\mathbf{F}_{pseudo,ptery}$ and $IL_{pseudo,ptery}$ are the muscle force and in-lever length, respectively, for the M. pseudotemporalis and M. pterygoideus collectively (Fig. 2E); and OL is the out-lever length measured from the jaw joint to the bite point (Fig. 2B–E). The forces acting at the jaw joints are important for maintaining the static equilibrium of the jaw mechanism by balancing the forces acting on the jaws (e.g. Sinclair and Alexander, 1987; Huber et al., 2008). However, because the goal of the present study was to evaluate jaw adductor muscle moments, these balancing forces were not reported.

Lastly, theoretical bite-force generation (BF) was calculated by doubling RBF to account for both the right and left jaw adductor musculature. This is consistent with other static bite-force models that assume simultaneous and maximum contraction of the adductor musculature during biting (e.g. Wainwright, 1987; Hernández and Motta, 1997; Van Daele et al., 2009; Curtis et al., 2010). We understand that this does not account for the full range of functional variation in muscle recruitment (De Vree and Gans, 1984; Gans et al., 1985; Cleuren et al., 1995). The ramifications of other values for muscle recruitment (80 and 90%) have been explored in an earlier study (Pfaller, 2009).

Size and rupture force of snails

The sizes of snails consumed by each *S. minor* (N=30) were determined by recovering intact opercula from the digestive tract. The maximum length of opercula (OpL) was measured from digital images (ImageJ v. 1.40), and snail sizes were reconstructed based on the relationship between OpL and maximum snail length (SnL) from a sample of 50 wild-caught snails. OpL was a strong predictor of SnL (t_{48}=26.3, r^2=0.94, P<0.0001: SnL=1.55+3.83OpL), and therefore was used as a proxy for estimating snail size.

Using a mechanical loading frame (model 312.31, MTS Corp., Eden Prairie, MN, USA), the rupture forces of *Goniobasis* snails were tested in the jaws of turtle specimens representing three different size classes (small, 85 g; medium, 174 g; large, 306 g). Two load cells were used in the mechanical loading frame to reduce error across scale: 250 N (model 41-0571-04-01, Sensotec, Brookfield, WI, USA) for the medium and small turtles, and 5000 N (model 661.19e-01, MTS Corp.) for the large turtles. Skulls from turtles used for biomechanical analyses were removed and aligned upside down in a custom-built frame, which braced the skull anteroposteriorly and mediolaterally. Additionally, the jaw joint was restrained to resist ventral disarticulation. For each turtle, a size series of live *Goniobasis* were aligned between the jaws so that the widest whorl contacted the flat crushing surfaces of the upper and lower rhamphotheci. This location represents the site along the jaw where *S. minor* processes snails (Pfaller, 2009), as well as the bite point where we measured and modeled bite forces. During a typical loading trial, compressive force was applied at a constant loading rate (0.5 mm s^{-1}) to the posteroventral surface of the mid-jaw symphysis until rupture of the snail was achieved. This created snail fragments that mimic those found in the digestive tracts in which typically only the first whorl was ruptured (Pfaller, 2009).

Statistical analysis

Except for descriptive statistics, pennation angles and MA, all data were logarithmically transformed for use in statistical analyses. Values for empirically derived and theoretical estimates of bite force were regressed (reduced major-axis regression, RMA) against skull length (SL). Modified t-tests were used to test for statistically supported differences in slope, and paired t-tests were used to compare theoretical and observed bite-force values.

Scaling relationships among biomechanical variables, and between biomechanical variables and bite force (observed), were determined from RMA and compared with null predictions based on isometric scaling (pennation angles and MA=0.0; morphometrics and levers=1.0; areas and forces=2.0; masses=3.0). The isometric scaling model is based on Euclidean geometry, in which increases in linear dimensions by n lead to corresponding increases in area measures by n^2 and volume (or mass) by n^3 (Hill, 1950; Schmidt-Nielson, 1984; Emerson and Bramble, 1993). RMA regressions on $\log_{10}$-transformed data yielded equations of the form:

$$\log y = \log a + b\log x\,, \quad (3)$$

where x is the independent variable, y is the dependent variable, a is the y-intercept and b is the scaling or regression coefficient (Sokal and Rohlf, 2000). The scaling coefficient describes the relative allometry or isometry of the relationship. Deviations from isometry (i.e. allometry) were considered significant if the predicted slopes fell outside the 95% confidence intervals of the observed slopes. P-values were corrected using modified t-tests to reflect differences from isometric predictions. Scaling coefficients significantly greater or less than those predicted by isometry were designated as positive or negative allometry, respectively.

To evaluate the dietary ontogeny of snail consumption, the mean size of snails found in the diet (estimated from OpL) was regressed against SL. The regression equation of rupture force on SnL was used to extrapolate the force necessary to rupture snails recovered from the digestive tracts of turtles, and the slope was compared with the isometric prediction of 2.0 (rupture force is a function of stress). For each turtle, the estimated rupture forces of the five largest snails found in the diet were averaged (ARF) and compared with bite force (observed and theoretical) using paired t-tests. Scaling coefficients (RMA) of ARF and bite force (observed and theoretical) against SL were compared using modified t-tests. Reduced major-axis regressions were done using RMA for Java v.1.21 (Bohonak and van der Linde, 2004), and all other statistics were done using R for Windows v. 2.8.1 (R Development Core Team, 2008). For all analyses, the alpha value was 0.05.

RESULTS

Morphology and theoretical bite-force generation

The M. add. mand. externus was the largest of all muscles in *S. minor* (~91% of total muscle mass). It also made the greatest contribution to total PCSA (~86%) and bite force (~98%) (Table 1). The M. add. mand. posterior and internus were both relatively small (1.6 and ~7.5% of total muscle mass, respectively) and contributed comparably little to bite-force generation (0.5 and ~1.1%, respectively) (Table 1). Scaling coefficients for observed and theoretical bite force scaled to SL were significantly different from the isometric scaling prediction of 2.0 and were not statistically different from each other (observed: slope=2.67, 95% CI=2.50–2.84; theoretical: slope=2.71, 95% CI=2.54–2.88). Observed bite-force values were on average less than the theoretical bite-force estimates

Table 1. Descriptive statistics for musculoskeletal variables and bite-force generation in *Sternotherus minor*

Muscle subdivision	Mass (g)	Fiber length (cm)	Pennation angle (deg)	PCSA (cm^2)	In-lever length (cm)	Theoretical bite force (N)
M. adductor mandibulae externus						
P. prof. α	1.10±0.18	0.77±0.04	43.0±0.55	0.80±0.10	0.99±0.06	22.89±2.84
	0.10–3.0	0.39–1.13	39.2–49.2	0.16–1.92	0.55–1.55	4.6–55.5
(% of total)	(45±3.3)			(32±3.8)		(30±3.3)
P. prof. β	0.13±0.023	0.51±0.026	33.4±0.49	0.19±0.03	0.99±0.06	5.43±0.86
	0.012–0.46	0.23–0.68	28.4–37.7	0.027–0.56	0.55–1.55	0.78–16.2
(% of total)	(6.4±2.1)			(7.5±2.4)		(6.7±2.1)
P. prof. γ	0.48±0.090	0.50±0.026	42.6±0.42	0.57±0.09	0.99±0.06	16.31±2.6
	0.04–1.41	0.24–0.70	38.7–46.6	0.096–1.58	0.55–1.55	2.8–45.7
(% of total)	(19±2.5)			(21±3.4)		(20±3.3)
P. supf.	0.38±0.072	0.51±0.030	39.7±0.80	0.45±0.06	0.99±0.06	12.86±1.72
	0.04–1.27	0.54–0.80	34.3–48.1	0.11–1.12	0.55–1.55	3.15–32.39
(% of total)	(15±2.0)			(18±2.3)		(15.8±2.1)
P. med.	0.12±0.023	0.61±0.030	n.a.	0.17±0.026	0.71±0.033	3.49±0.53
	0.013–0.40	0.40–0.90		0.033–0.48	0.45–0.99	0.78–8.87
(% of total)	(5.5±1.1)			(7.0±1.4)		(9.2±1.2)
M. adductor mandibulae posterior						
M. post.	0.03±0.005	0.058±0.027	n.a.	0.04±0.006	0.36±0.017	0.52±0.063
	0.004–0.12	0.35–0.90		0.01–0.16	0.23–0.51	0.13–1.62
(% of total)	(1.6±0.07)			(1.9±0.07)		(0.5±0.002)
M. adductor mandibulae internus						
M. pseudo.	0.11±0.017	0.45±0.027	n.a.	0.20±0.026	0.14±0.007	0.85±0.11
	0.011–0.30	0.030–0.92		0.035–0.50	0.071–0.20	0.13–1.9
(% of total)	(5.0±0.12)			(8.4±0.19)		(0.83±0.003)
M. ptery.	0.05±0.008	0.46±0.020	n.a.	0.093±0.01	0.14±0.007	0.38±0.041
	0.007–0.18	0.28–0.65		0.021–0.28	0.071–0.20	0.082–1.08
(% of total)	(2.5±0.12)			(3.9±0.11)		(0.3±0.0008)

Values are the mean ± s.e.m. (top), minimum–maximum (middle) and mean percentage ± s.e.m. (bottom).

P. prof. α, Pars profunda α; P. prof. β, Pars profunda β; P. prof. γ, Pars profunda γ; P. supf., Pars superficialis; P. med., Pars media; M. post., M. posterior; M. pseudo., M. pseudotemporalis; M. ptery., M. pterygoideus.

Pertinent data not displayed are descriptive statistics for skull length (mean ± s.e.m.: 3.66±0.19 cm, range: 2.22–5.52 cm), observed bite force (mean ± s.e.m.: 55.0±7.28 N, range: 7.09–124.6 N), out-lever length (mean ± s.e.m.: 1.76±0.11 cm, range: 0.96–2.68 cm), resolved in-lever length (mean ± s.e.m.: 0.85±0.19 cm, range: 0.45–1.34 cm) and mechanical advantage (mean ± s.e.m.: 0.48±0.02, range: 0.44–0.51).

Table 2. Scaling of levers and mechanical advantage

Independent variables	r^2	Intercept (*a*)	Slope (*b*)	Lower limit	Upper limit	*P*-value	Isometric prediction	Growth type
(A) In-lever length against out-lever length								
$IL_{sup,pro}$	0.99	–0.25	1.01	0.98	1.04	0.25	1.0	I
IL_{med}	0.92	–0.13	0.80	0.72	0.88	<0.0001	1.0	N
IL_{post}	0.96	0.18	0.78	0.72	0.84	<0.0001	1.0	N
$L_{pseudo,ptery}$	0.96	0.63	0.76	0.70	0.82	<0.0001	1.0	N
RIL	0.97	–0.36	1.01	0.97	1.05	0.32	1.0	I
(B) Mechanical advantage against skull length								
MA	0.84	0.39	0.045	–0.019	0.109	0.07	0.0	I

(A) Resolved in-lever length and in-lever lengths for isolated jaw adductor muscles scaled against out-lever length, and (B) mechanical advantage against skull length in *Sternotherus minor*. Significance level (α=0.05). *P*-values were corrected using modified *t*-tests to reflect differences from isometric predictions.
For growth types, I=isometry and N=negative allometry. $IL_{sup,pro}$, Pars superficialis and Pars profunda in-lever length; IL_{med}, Pars media in-lever length; IL_{post}, M. posterior in-lever length; $IL_{pseudo,ptery}$, M. pseudotemporalis and M. pterygoideus in-lever length; RIL, resolved in-lever length; OL, out-lever length; MA, mechanical advantage.

(t_{29}=3.42, *P*=0.0019). However, relative to other comparisons, this difference was only marginally significant.

Scaling of feeding biomechanics

$IL_{sup,pro}$ scaled isometrically relative to OL, while IL_{med}, IL_{post} and $IL_{pseudo,ptery}$ scaled with negative allometry relative to OL (Table 2A). Resolved in-lever length (RIL) scaled isometrically relative to OL (Table 2A and Fig. 3A), and MA (RIL:OL) scaled isometrically relative to SL (Table 2B and Fig. 3B).

Changes in muscle mass of isolated muscle subdivisions in most cases scaled with positive allometry relative to SL (Table 3A). The two exceptions were the M. posterior and M. pterygoideus, which scaled isometrically (Table 3A). In addition, total muscle mass scaled with positive allometry relative to SL (Table 3A and Fig. 4A). Observed bite force scaled with positive allometry relative to the masses of each isolated muscle subdivision (Table 3B) and to the total muscle mass (Table 3B and Fig. 4B).

Fiber lengths and fiber angles of the Pars superficialis and Pars profunda (α, β and γ) in most cases scaled with negative allometry and positive allometry, respectively, relative to their respective muscle masses (Table 4A,B and Fig. 5). Moreover, fiber lengths of M. posterior, M. pseudotemporalis and M. pterygoideus scaled isometrically relative to their respective muscle masses, and the fiber lengths of Pars media scaled with negative allometry relative to

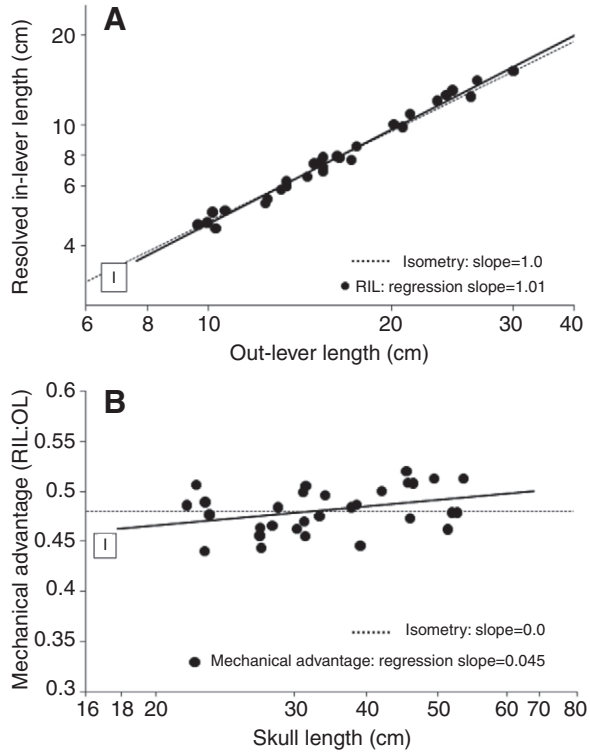

Fig. 3. Scaling of levers and mechanical advantage. (A) A log–log plot of resolved in-lever length (RIL) scaled against out-lever length (OL) and (B) mechanical advantage (RIL:OL) scaled against skull length in *S. minor*. Solid lines, reduced major axis regressions for the data; dotted lines, scaling predictions based on isometric growth set to cross data lines at the mean values of each independent variable. I=isometry.

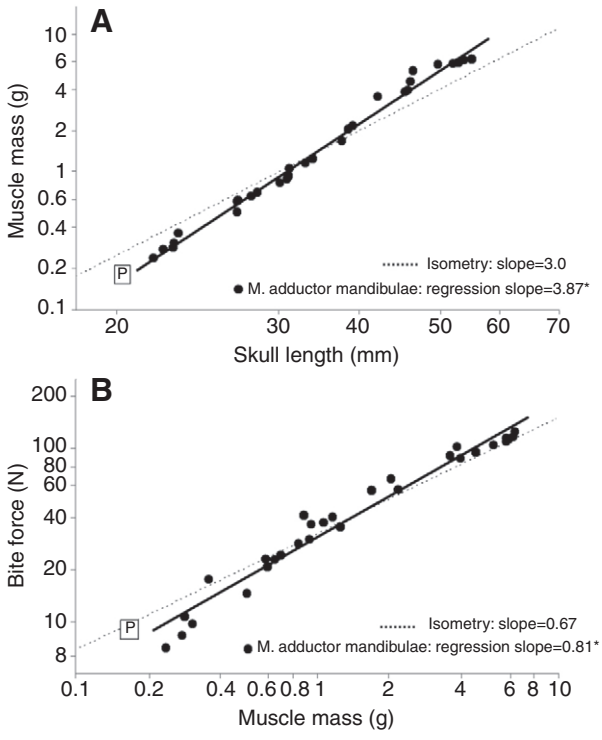

Fig. 4. log–log plots for (A) scaling of total M. adductor mandibulae mass on skull length, and (B) scaling of bite force on total M. adductor mandibulae mass in *S. minor*. Solid lines, reduced major axis regressions for the data; dotted lines, scaling predictions based on isometric growth set to cross data lines at the mean value of each independent variable. P=positive allometry. Asterisk indicates slope that is significantly different from isometry.

Table 3. Scaling of muscle masses

Independent variables	r^2	Intercept (*a*)	Slope (*b*)	Lower limit	Upper limit	*P*-value	Isometric prediction	Growth type
(A) Muscle mass against skull length								
P. prof. α	0.97	–4.25	3.90	3.66	4.14	<0.0001	3.0	P
P. prof. β	0.94	–4.96	3.79	3.43	4.15	<0.0001	3.0	P
P. prof. γ	0.98	–5.04	4.17	3.93	4.41	<0.0001	3.0	P
P. supf.	0.95	–4.87	4.01	3.67	4.35	<0.0001	3.0	P
P. med.	0.95	–4.90	3.73	3.41	4.05	<0.0001	3.0	P
M. post.	0.89	–3.59	3.18	2.78	3.57	0.185	3.0	I
M. pseudo.	0.96	–3.50	3.45	3.18	3.72	0.001	3.0	P
M. ptery.	0.92	–3.26	3.09	2.76	3.42	0.30	3.0	I
Total mass	0.98	–3.85	3.87	3.66	4.09	<0.0001	3.0	P
(B) Bite force against muscle mass								
P. prof. α	0.97	0.16	0.78	0.75	0.85	<0.0001	0.67	P
P. prof. β	0.92	0.85	0.82	0.73	0.91	0.001	0.67	P
P. prof. γ	0.94	0.54	0.75	0.68	0.82	0.013	0.67	P
P. supf.	0.93	0.56	0.78	0.70	0.86	0.0035	0.67	P
P. med.	0.91	0.87	0.84	0.74	0.94	0.0007	0.67	P
M. post.	0.89	0.30	0.98	0.85	1.11	<0.0001	0.67	P
M. pseudo.	0.93	–0.07	0.91	0.82	1.00	<0.0001	0.67	P
M. ptery.	0.86	0.067	1.01	0.87	1.15	<0.0001	0.67	P
Total mass	0.96	–0.129	0.81	0.75	0.87	<0.0001	0.67	P

(A) Total and isolated muscle mass against skull length, and (B) bite-force generation (observed) against total and isolated muscle mass in *S. minor*. Significance level (α=0.05). *P*-values were corrected using modified *t*-tests to reflect differences from isometric predictions.

For growth types, P=positive allometry and I=isometry. P. prof. α, Pars profunda α; P. prof. β, Pars profunda β; P. prof. γ, Pars profunda γ; P. supf., Pars superficialis; P. med., Pars media; M. post., M. posterior; M. pseudo., M. pseudotemporalis; M. ptery., M. pterygoideus.

muscle mass (Table 4A). PCSA of each isolated muscle subdivision scaled with positive allometry relative to SL, except PCSA of M. posterior, which scaled isometrically (Table 4C). Total PCSA of the M. add. mand. scaled with positive allometry relative to SL (Table 4C and Fig. 6A).

Bite force scaled with positive allometry relative to the PCSA of Pars profunda α, M. posterior, M. pseudotemporalis and M. pterygoideus, and isometically relative to the PCSA of Pars profunda β and γ, Pars superficialis and Pars media (Table 4D). Bite force scaled isometrically relative to the total PCSA of M. add. mand. (Table 4D and Fig. 6B).

Size and rupture force of snails

Three-hundred and eighty-two snail opercula were recovered from the digestive tracts of the 30 turtle specimens. There was a highly correlated, positive exponential relationship between the mean SnL (estimated from OpL) and turtle SL (r^2=0.89, SL=2.797e$^{0.0357SnL}$; Fig. 7A). Seventy-seven out of 113 snails tested in the mechanical loading frame were successfully ruptured [small turtle (*N*=18 snails: range 4.52–10.15 mm), medium turtle (*N*=29 snails: range 4.85–18.02 mm), large turtle (*N*=30 snails: range 15.03–26.98 mm)]. Thirty-six trials were excluded from *post hoc* analyses because these snails either slipped within the jaws or ruptured in a biologically uncharacteristic manor (i.e. catastrophic rupture of the entire shell). When data from all three turtle size classes were combined, a significant positive relationship between the rupture force and SnL was revealed (RMA: r^2=0.76, t_{75}=19.32, *P*<0.0001: rupture force=13.106SnL–60.09). In addition, rupture force scaled isometrically relative to SnL (RMA on log–log data: regression slope=1.77, r^2=0.72, t_{75}=1.53, *P*=0.07). The regression slope of ARF *versus* SL was significantly greater than the isometric scaling prediction of 2.0 (t_{29}=2.81, *P*=0.0044; Fig. 7B) and was not statistically different from the regression slopes of theoretical bite force (t_{29}=1.437, *P*=0.081) or observed bite force (t_{29}=1.197, *P*=0.121) scaled to SL (Fig. 7B). Moreover, ARF values were significantly greater than the theoretical bite forces (t_{29}=8.85, *P*<0.0001) and observed bite forces (t_{29}=9.50, *P*<0.0001) for each turtle (Fig. 7B).

DISCUSSION

To our knowledge, this study is the first to utilize static bite-force modeling to determine which musculoskeletal features are responsible for allometric increases in bite force across ontogeny in a tetrapod vertebrate. Although our model of bite-force generation for *S. minor* tends to slightly overestimate observed bite-force values, it accurately predicts the scaling of bite force across ontogeny. The inconsistency in absolute terms is likely to be the result of our assumptions for muscle stress (25 N cm^{-2}) and recruitment (100%), which were estimated because experimentally derived values are currently unavailable for chelonian cranial muscles. Recent work that tested the ramifications of a range of values for muscle stress (20, 25 and 30 N cm^{-2}) and recruitment (80, 90 and 100%) indicates that two combinations of these values (30 N cm^{-2} with 80% and 25 N cm^{-2} with 90%) generate static bite-force estimates that are statistically identical to the observed values (Pfaller, 2009). Nevertheless, the static model accurately predicts the scaling of bite force, which suggests that the underlying morphology of the musculoskeletal system is a good predictor of observed performance and that ontogenetic changes in biting motivation are negligible. Furthermore, it implies that the biomechanical theory used to develop the model is sound. From these results, we were able to explore the scaling relationships between musculoskeletal growth, bite-force generation and dietary ontogeny.

Relationship between musculoskeletal growth and bite-force generation

Bite-force generation in *S. minor* scales with positive allometry relative to SL. All previous studies across a broad range of durophagous taxa, including *S. minor* (Pfaller et al., 2010), show a similar pattern of significant positive allometry of bite force relative to body and head dimensions through ontogeny (Herrel and Gibb, 2006). The consistency of this pattern has provided the impetus for

Table 4. Scaling of jaw muscle architecture and physiological cross-sectional area

Independent variables	r^2	Intercept (*a*)	Slope (*b*)	Lower limit	Upper limit	*P*-value	Isometric prediction	Growth type
(A) Fiber length against muscle mass								
P. prof. α	0.94	1.38	0.27	0.24	0.30	<0.0001	0.34	N
P. prof. β	0.73	1.41	0.30	0.24	0.36	0.09	0.34	I
P. prof. γ	0.87	1.32	0.26	0.22	0.30	<0.0001	0.34	N
P. supf.	0.91	1.29	0.29	0.26	0.32	0.003	0.34	N
P. med.	0.87	1.55	0.25	0.22	0.28	<0.0001	0.34	N
M. post.	0.83	1.36	0.29	0.24	0.34	0.019	0.34	I
M. pseudo.	0.68	1.08	0.30	0.24	0.36	0.110	0.34	I
M. ptery.	0.61	1.22	0.28	0.21	0.35	0.0394	0.34	I
(B) Pennation angle against muscle mass								
P. prof. α	0.86	1.52	0.062	0.054	0.070	<0.0001	0.0	P
P. prof. β	0.78	1.46	0.075	0.061	0.089	<0.0001	0.0	P
P. prof. γ	0.59	1.56	0.046	0.036	0.056	<0.0001	0.0	P
P. supf.	0.84	1.47	0.094	0.080	0.110	<0.0001	0.0	P
(C) PCSA against skull length								
P. prof. α	0.95	–2.43	2.73	2.51	2.95	<0.0001	2.0	P
P. prof. β	0.84	–3.17	2.79	2.37	3.21	0.0007	2.0	P
P. prof. γ	0.95	–3.18	3.09	2.83	3.35	<0.0001	2.0	P
P. supf.	0.91	–2.64	2.70	2.40	3.0	<0.0001	2.0	P
P. med.	0.92	–3.33	2.86	2.56	3.16	<0.0001	2.0	P
M. post.	0.82	–2.07	2.36	1.98	2.74	0.067	2.0	I
M. pseudo.	0.88	–1.90	2.65	2.31	2.99	0.0006	2.0	P
M. ptery.	0.83	–1.95	2.46	2.08	2.84	0.021	2.0	P
Total	0.97	–1.92	2.73	2.55	2.91	<0.0001	2.0	P
(D) Bite force against PCSA								
P. prof. α	0.97	–0.45	1.15	1.07	1.23	0.0004	1.0	P
P. prof. β	0.79	0.32	1.12	0.92	1.32	0.120	1.0	I
P. prof. γ	0.89	–0.01	1.01	0.89	1.13	0.434	1.0	I
P. supf.	0.89	–0.18	1.08	0.94	1.22	0.131	1.0	I
P. med.	0.87	0.40	1.09	0.93	1.25	0.135	1.0	I
M. post.	0.79	–0.49	1.33	1.11	1.55	0.0027	1.0	P
M. pseudo.	0.85	–0.99	1.18	1.02	1.36	0.0160	1.0	P
M. ptery.	0.74	–0.77	1.27	1.03	1.51	0.0160	1.0	P
Total mass	0.93	–1.023	1.09	0.97	1.33	0.163	1.0	I

(A) Mean fiber length against isolated muscle mass, (B) mean pennation angle against isolated muscle mass, (C) isolated and total physiological cross-sectional area against skull length, and (D) bite-force generation (observed) against isolated and total physiological cross-sectional area in *S. minor*.

Significance level (α=0.05). *P*-values were corrected using modified *t*-tests to reflect differences from isometric predictions.

For growth types, P=positive allometry, I=isometry and N=negative allometry. P. prof. α, Pars profunda α; P. prof. β, Pars profunda β; P. prof. γ, Pars profunda γ; P. supf., Pars superficialis; P. med., Pars media; M. post., M. posterior; M. pseudo., M. pseudotemporalis; M. ptery., M. pterygoideus; PCSA, physiological cross-sectional area.

investigators to elucidate which biomechanical factors are responsible for the allometric patterns of force production. Although ontogenetic studies on the scaling of functionally relevant musculoskeletal properties are few, the available data indicate mixed results among vertebrates. Studies in fishes show that positive allometry in observed and theoretical bite force can be attributed to both positive allometry in MA without changes to muscle PCSA (Grubich, 2005; Huber et al., 2008) and positive allometry in MA in combination with allometric increases in muscle PCSA (Wainwright, 1987; Hernández and Motta, 1997; Herrel et al., 2005; Huber et al., 2006; Kolmann and Huber, 2009). In the latter, positive allometry in PCSA was achieved both by changes in muscle size without changes in muscle architecture (Wainwright, 1987) and by changes in muscle architecture without changes in muscle size (Herrel et al., 2005). Moreover, in finches, bite-force positive allometry was proportional to allometric changes in jaw muscle size (Van der Meij and Bout, 2004). The scaling of feeding biomechanics in *S. minor* investigated in this study shows a somewhat different combination of results. We found that *S. minor* achieves a relative increase in bite force across ontogeny through the combined effects of increasing muscle size and changing muscle architecture, but not by enhancing MA. Muscle hypertrophy alone did not account for all ontogenetic changes in bite force in *S. minor*, as bite force scaled with positive allometry relative to muscle mass (total and isolated subdivisions). Instead, we found that muscular hypertrophy was associated with an increase in the mean pennation angle and a decrease in the mean fiber length. These parameters, which covary in pennate muscles (Gans and DeVree, 1987), acted in concert to increase the total PCSA of the adductor musculature, such that changes in PCSA were proportional to bite force. Each of these analyses ultimately shows positive allometry in bite-force generation, yet the scaling of biomechanical properties is not always the same. This suggests that because the feeding apparatus in vertebrates is composed of a complex and integrated set of musculoskeletal structures, ontogenetic increases in bite force are not constrained to one universal pattern of morphological modification. While studies in fishes are numerous, broader phylogenetic sampling among tetrapods would provide the opportunity to assess these phenomena in a more functionally diverse and evolutionary framework.

The suite of musculoskeletal changes related to allometric increases in bite force in *S. minor* may result from the turtles' need to retract their heads between the margins of their shell as an antipredation tactic while at the same time allowing for feeding on

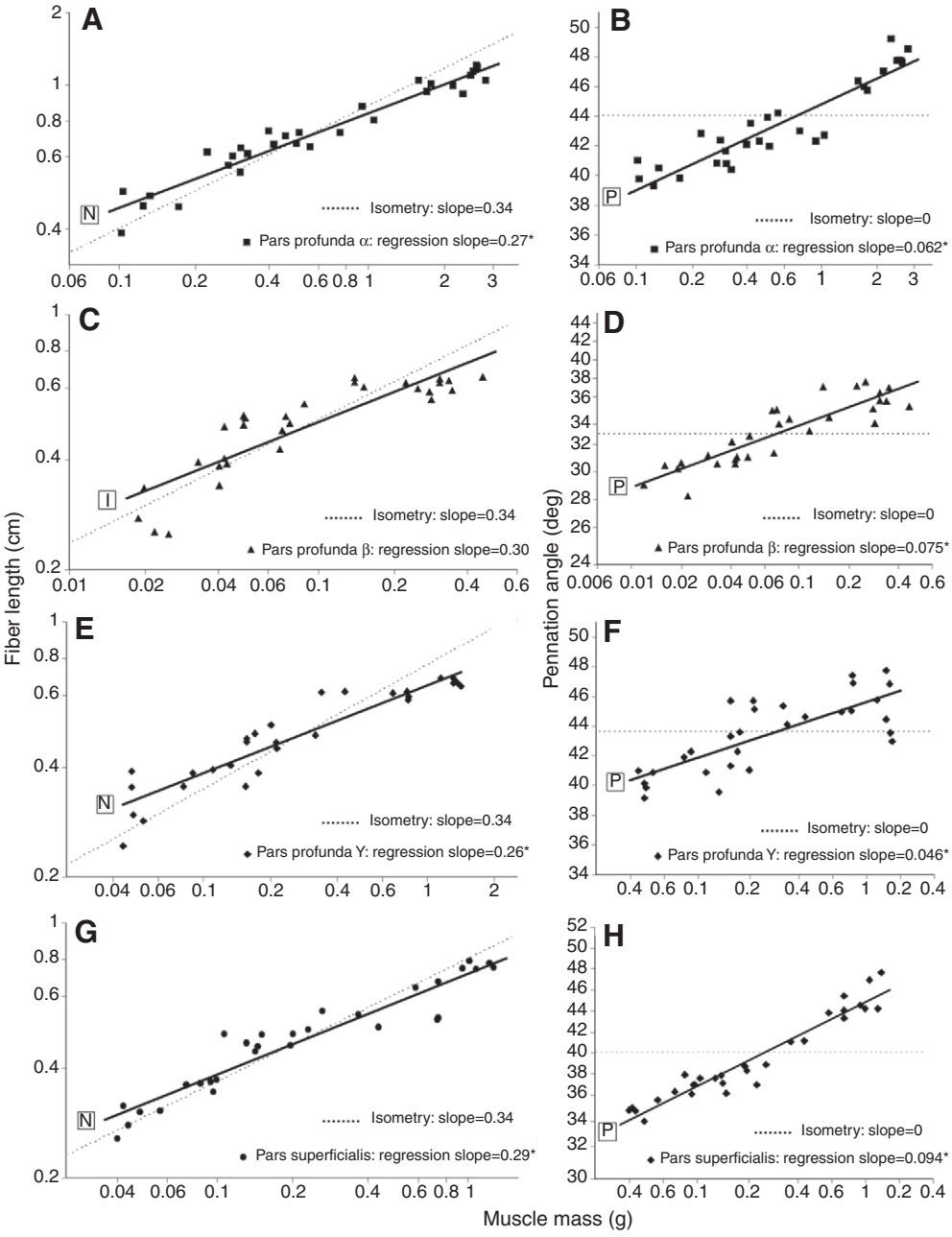

Fig. 5. log–log plots for the scaling of fiber lengths and pennation angles on isolated muscle masses of the M. adductor mandibulae externus in *S. minor*. Solid lines, reduced major axis regressions for the data; dotted lines, scaling predictions based on isometric growth set to cross data lines at the mean value of each independent variable. (A,B) Pars profunda α, (C,D) Pars profunda β, (E,F) Pars profunda γ and (G,H) Pars superficialis. P=positive allometry, N=negative allometry, I=isometry. Asterisk indicates slope that is significantly different from isometry.

durable prey (Dalrymple, 1979; Herrel et al., 2002). Notably, bite forces in some fishes are collectively generated by several adductor muscles (e.g. Huber et al., 2006), whereas in *S. minor* they are almost entirely generated by the M. add. mand. externus (~91% of the total adductor muscle mass). This muscle also accounts for approximately 73 and 88% of the adductor muscle mass in the turtles *Apalone* (=*Trionyx*) *ferox* (Dalrymple, 1979) and *Chrysemys picta* (Sinclair and Alexander, 1987), respectively. The prominence of the M. add. mand. externus in turtles is likely related to its position within the posterior half of the head and the need to maintain limits on head size for retraction (Dalrymple, 1979). The attachment site for this muscle, the external tendon, runs dorsally from the lower jaw to the trochlear process where it is redirected posteriorly towards the back of the head (Fig. 2). This rather unique 'pulley' system allows turtles to position the bulk of this muscle along the dorsocaudal crania without losing substantial mechanical advantage. Moreover, the multipennate arrangement of the M. add. mand. externus in *S. minor* (Fig. 2) dramatically elevates the PCSA of the adductor musculature and capacity of bite-force generation. Multipennation of the M. add. mand. externus has been found in other turtles with high bite forces (trionychids and *Podocnemis*) (Schumacher, 1973). The development of a multipennate muscle-fiber arrangement from the more common bipennate pattern seen in most turtles (Schumacher, 1973) allows durophagous turtles to increase the force-generating capacity of their adductor muscles without dramatically increasing the muscle size. Thus, the allometric patterns of growth among muscle masses in *S. minor*, as well as their fiber architecture, reflect an emphasis on maximizing the PCSA of the M. add. mand. externus (Pars superficialis and Pars profunda α, β, γ). These growth patterns facilitate increases in the capacity for bite-force generation without substantial increases in head height and depth, while simultaneously retaining the capacity for head retraction.

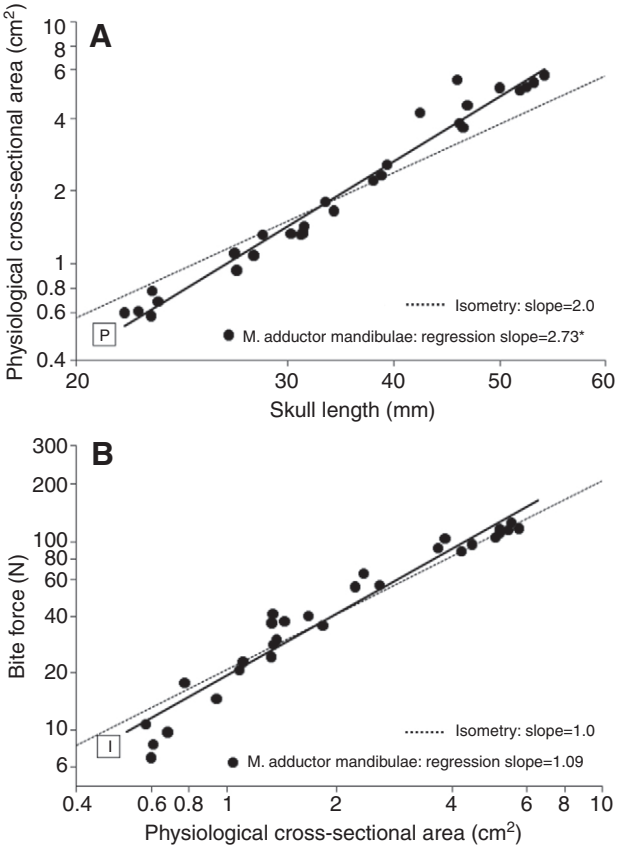

Fig. 6. log–log plots for (A) scaling of total M. adductor mandibulae physiological cross-sectional area on skull length and (B) bite force on total M. adductor mandibulae physiological cross-sectional area in *S. minor*. Solid lines, reduced major axis regressions for the data; dotted lines, scaling predictions based on isometric growth set to cross data lines at the mean value of each independent variable. P=positive allometry, I=isometry. Asterisk indicates slope that is significantly different from isometry.

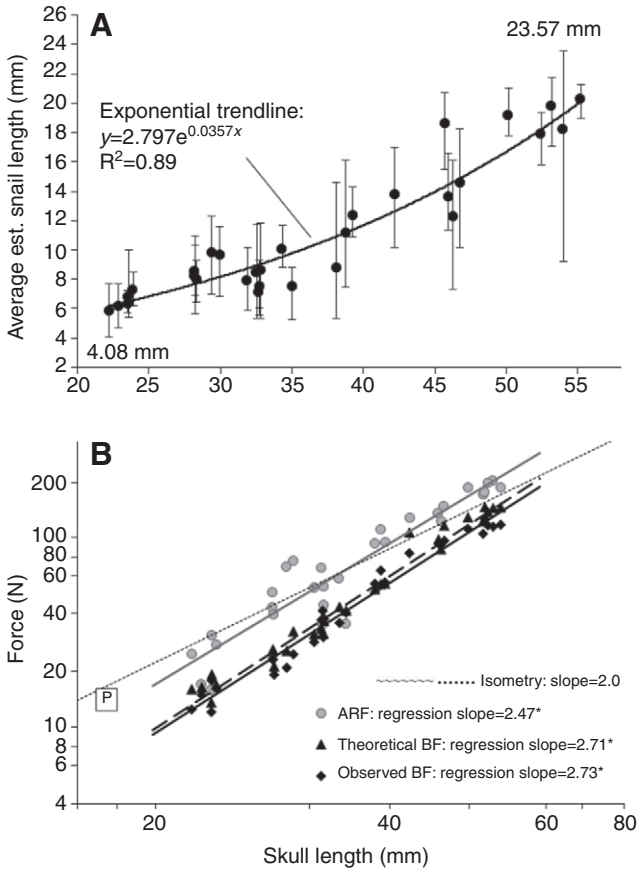

Fig. 7. Size and rupture forces of snails. (A) Mean length of all snails found in the digestive tract estimated from operculum length. Bars on the data points represent the estimated minimum and maximum size of snails found in the diet of each turtle. (B) log–log plot for the average force required to rupture the five largest snails per turtle (ARF; gray circles and line), observed bite force (black diamonds, black line) and theoretical bite force (black triangles, dashed line). Dotted line represents the scaling predictions based on isometric growth set to cross data lines at the mean value of ARF. P=positive allometry. Asterisk indicates slope that is significantly different from isometry.

Hypothetically, if we manipulate our model to simulate two different muscle-fiber arrangements for the M. add. mand. externus, one bipennate and one multipennate, the bipennate muscle would need to be ~3 times the mass of the multipennate muscle to generate the same amount of force. Under this scenario, the accommodation of such a muscle mass would dramatically increase head size and almost certainly limit the capacity for head retraction. This demonstrates the importance of multipennation for muscle-force generation and the maintenance of muscle mass in size-restricted musculoskeletal feeding systems.

For *S. minor*, however, this morphology does not come without a potential cost. Biomechanical theory predicts that a musculoskeletal apparatus that is proficient at generating high forces will forfeit the ability to generate high speed at multiple anatomical levels (Cochran, 1982; Herrel et al., 2009). Lever systems with high force transmission (i.e. high MA) are typically characterized by relatively short out-levers, whereas those suited for rapid movements utilize relatively long out-levers (i.e. low MA) (Herrel et al., 2002). Among studies of turtles, measurements of MA are restricted to the M. add. mand. externus for biting at the tip of the jaws (Dalrymple, 1979): ~0.30 for a species that feeds on fast, elusive prey (e.g. *Deirochelys*) and ~0.38 in a more omnivorous species (e.g. *Apalone*). A comparable measurement of MA for *S. minor* in this study is ~0.52 (adjusted from ~0.56 for only M. add. mand. externus at the bite point), suggesting a greater emphasis on force production in *S. minor*. At the muscular level, pennate-fiber arrangements with high PCSA are capable of slow, forceful contractions, whereas parallel-fiber arrangements are capable of fast, lower force movements with the greater range of contraction (Gans and Bock, 1965; Cochran, 1982; Gans et al., 1985). For these reasons, it seems that the evolution of high bite force required for durophagy in *S. minor* has come at the expense of jaw-closing speed and therefore the ability to feed on fast, elusive prey. Particularly in adult *S. minor*, fast jaw-closing behaviors associated with suction feeding are poorly developed (Pfaller, 2009), and elusive prey (i.e. fish) are rarely found in the diet (Tinkle, 1958). Further comparative studies between piscivorous and durophagous turtles would be particularly enlightening in the context of functional tradeoffs between generating force and speed in musculoskeletal feeding systems.

Relationship between bite-force generation and durophagy

For *S. minor*, the ecological significance for multipennate jaw adductors and positive allometry in bite force is related to the

consumption of disproportionately larger *Goniobasis* snails during ontogeny. Mollusk shell is among the hardest and densest of biological materials and, coupled with the thick-walled, domed architecture, makes snail shells among the structurally strongest biological entities (Currey, 1980). Because mechanical failure of these structures requires the application of substantial compressive and shear forces (Vermeij, 1987), the consumption of larger snails necessitates the development of relatively higher bite forces. These results are consistent with the findings of numerous studies across a broad range of durophagous taxa, in which larger individuals develop relatively greater bite forces, and tend to consume relatively larger and more durable prey (e.g. Kiltie, 1982; Herrel et al., 2001; Erickson et al., 2003; Grubich, 2005; Kolmann and Huber, 2009). For *S. minor*, allometric patterns of growth and performance that facilitate access to relatively larger snails likely confer either a competitive or energetic advantage over isometric patterns. Competition with sympatric species and smaller conspecifics is likely minimal because the density of snails in these lotic systems is typically very high (>300 snails m^{-2}) (Berry, 1975). Alternatively, positive allometry may provide an energetic advantage in which larger individuals can increase their net rate of energy intake when foraging (optimal foraging) (MacArthur and Pianka, 1966). Presumably, as snail volume will increase as the cube of snail length (Hill, 1950; Schmidt-Nielson, 1984), by consuming larger snails adult *S. minor* would need to ingest fewer snails to meet its minimum energy requirements (Dalrymple, 1977). Moreover, larger turtles with higher bite forces may require less handling time to consume snails of certain sizes (Herrel et al., 2001; Verwaijen et al., 2002; Van der Meij and Bout, 2006). Together these energetic benefits may favor allometric patterns of growth and performance over isometric patterns, and allow *S. minor* to maintain or exceed its minimum foraging requirements as it grows.

Numerous studies have sought to establish the causal relationships between prey-crushing forces and bite forces across ontogeny (e.g. Herrel et al., 2001; Wyckmans et al., 2007; Kolmann and Huber, 2009), yet few have directly compared individual bite forces and the forces needed to rupture specific prey items found in the diet (Wainwright, 1987; Hernández and Motta, 1997; Grubich, 2005). In the present study, we found that the allometry of bite force in *S. minor* increases with the same scaling relationship as the average rupture forces of the largest snails found in the diet. Similar results have been shown among durophagous fishes (Wainwright, 1987; Hernández and Motta, 1997; Grubich, 2005). These results indicate that during growth individuals are feeding near the mechanical limits of their dietary options. Because durophagous taxa cannot consume prey items that they cannot crush, individuals are trophically constrained during growth by the absolute bite forces that can be generated by their musculoskeletal feeding apparatus (Hernández and Motta, 1997). These results provide empirical evidence that the allometric patterns of adductor muscle size and architecture in *S. minor* are developmentally linked to the structural properties of their primary prey. This correlation and its potentially broader evolutionary implications are important for understanding the mechanistic and functional issues that underlie the evolution of phenotypic traits (Arnold, 1983; Kingsolver and Huey, 2003; Schwenk and Wagner, 2004).

Interestingly, however, despite having similar scaling relationships, the forces required to rupture snails in this study were absolutely greater than the bite forces generated by *S. minor*. Similar results were found for the aforementioned mollusk-crushing fishes (Wainwright, 1987; Hernández and Motta, 1997; Grubich, 2005). These results superficially complicate the conclusions that can be drawn from bite-force testing and biomechanical modeling because the tight relationship between the musculoskeletal morphology and bite-force generation apparently does not match the ecological requirements. However, when processing durable prey, durophagous taxa rarely rupture their largest prey with a single load; instead, they typically exhibit several discrete crushing efforts, in which the prey item is loaded and repositioned several times until it is successfully ruptured or abandoned. This behavior for mollusk crushing is exhibited by *S. minor* (Pfaller, 2009), as well as durophagous fishes (Wainwright, 1987; Hernández and Motta, 1997; Grubich, 2005), lizards (Gans et al., 1985) and turtles (Dalrymple, 1977). Consequently, *S. minor* may rupture relatively small snails with a single load similar to our mechanical-loading trials, while rupture of larger snails is likely achieved with repeated, subcritical loads. Multiple bite-force loadings may allow *S. minor* to exploit mechanical weaknesses (cracks or spalls) caused during previous loads that compromise the structural integrity of the snail shell, so that large snails ultimately rupture at lower compressive and shear forces. These weak points would act as stress concentrators that allow turtles to rupture large snails which are apparently outside the range of their bite-force capacity. Preliminary mechanical-loading tests, in which snails were loaded to subcritical forces (i.e. the observed bite forces of *S. minor*), did induce spalling and subsequent rupture, thus supporting this hypothesis. While more work is needed to test the ecological importance of such behaviors for durophagous species, these results indicate that behavior plays an integral and often neglected role in the classic ecomorphological paradigm between morphology, performance and ecology (Arnold, 1983; Kingsolver and Huey, 2003).

CONCLUSIONS

In the durophagous turtle *S. minor*, we found that allometric scaling of the major jaw adductor muscle mass and degree of muscle pennation lead to relative increases in bite-force generation that facilitate changes in prey robustness across ontogeny. First, we statically modeled bite forces to accurately predict the scaling of bite-force generation across ontogeny and identified the musculoskeletal traits that were responsible for allometric changes in bite-force generation. Second, we used a mechanical-loading frame to test the rupture forces of snails found in the diet and established a direct scaling relationship between bite-force generation and dietary forces. These results show that (1) the underlying morphology of the musculoskeletal system is a good predictor of observed performance, and the biomechanical theory used to develop the predictions is sound, (2) bite-force positive allometry in *S. minor* is accomplished by augmenting muscle size and muscle pennation, but not mechanical advantage, (3) multipennate fiber arrangements are important for high muscle-force generation and the maintenance of muscle size, and (4) access to larger, more robust prey items is likely accomplished through a coupling of relatively high bite-force capacity and specific feeding behaviors. For durophagous taxa, such as *S. minor*, positive allometry of bite-force generation is directly linked to the scaling of musculoskeletal traits and is a major determinant for patterns of resource use (Wainwright, 1987; Kolmann and Huber, 2009). By developing greater bite forces that increase proficiency in crushing larger, more durable prey, durophagous animals may increase the net rate of energy intake when foraging (optimal foraging) (MacArthur and Pianka, 1966) and presumably enhance their fitness (Anderson et al., 2008). Consequently, studies similar to the one presented here are imperative for understanding the mechanistic and

functional issues that underlie the evolution of phenotypic traits (Arnold, 1983; Kingsolver and Huey, 2003).

LIST OF SYMBOLS AND ABBREVIATIONS

Anatomy	
M. add. mand.	Musculus adductor mandibulae
M. post.	Musculus posterior
M. pseudo.	Musculus pseudotemporalis
M. ptery.	Musculus pterygoideus
P. prof. α	Pars profunda α
P. prof. β	Pars profunda β
P. prof. γ	Pars profunda γ
P. sup.	Pars superficialis
PCSA	physiological cross-sectional area
SL	skull length
θ	muscle pennation angle
Mechanics	
BF	bite force
BF_{med}	bite force generated by the Pars media
BF_{post}	bite force generated by the M. posterior
$BF_{pseudo,ptery}$	bite force generated by the M. pseudotemporalis and M. pterygoideus
$BF_{sup,pro}$	bite force generated by the Pars superficialis and Pars profunda (α, β, γ)
$\mathbf{F}$	muscle force
$\mathbf{F}_{med}$	force generated by the Pars media
$\mathbf{F}_{post}$	force generated by the M. posterior
$\mathbf{F}_{pseudo,ptery}$	force generated by the M. pseudotemporalis and M. pterygoideus
$\mathbf{F}_{sup,pro}$	force generated by the Pars superficialis and Pars profunda (α, β, γ)
IL	in-lever length
IL_{med}	in-lever length of the Pars media
IL_{post}	in-lever length of the M. posterior
$IL_{pseudo,ptery}$	in-lever length of the M. pseudotemporalis and M. pterygoideus
$IL_{sup,pro}$	in-lever length of the Pars superficialis and Pars profunda (α, β, γ)
J	jaw joint
MA	mechanical advantage (RIL:OL)
OL	out-lever length
RBF	right-side bite force
RIL	resolved in-lever length
Statistics and regression	
a	regression intercept
b	regression slope (scaling coefficient)
CI	confidence interval
r^2	coefficient of determination
RMA	reduced major-axis regression
α	significance level
Other	
ARF	average force required to rupture the five largest snails found in the diet of each turtle
I	isometry
N	negative allometry
OpL	snail operculum length
P	positive allometry
SnL	snail length

ACKNOWLEDGEMENTS

We would like to thank Nathanael Herrera, Kenneth Wray and Pierson Hill for assistance in the field: catching turtles, collecting data and providing valuable scientific guidance. Robert Walsh (National High Magnetic Field Laboratory, FSU), Daniel Baxter (Department of Physics, FSU) and Lou Pfoul (Kistler Inc.) helped design and construct the bite-force transducer. Many thanks to Peter Meylan and the Eckerd College Herpetology Club for allowing us to participate in the Rainbow Run turtle surveys, and for catching many of the turtles used in this research. Dave Kralovanec and the Rainbow River Animal Hospital humanely killed the specimens for this study. Support for this research was provided by the Department of Biological Science at Florida State University. Lastly, we would like to thank the Florida Department of Environmental Protection and the staff of Rainbow Springs State Park for allowing us to conduct this research.

REFERENCES

Anderson, R. A., McBrayer, L. D. and Herrel, A. (2008). Bite force in vertebrates: opportunities and caveats for use of a nonpareil whole-animal performance measure. *Biol. J. Linn. Soc.* **93**, 709-720.
Arnold, S. J. (1983). Morphology, performance, and fitness. *Am. Zool.* **23**, 347-361.
Berry, J. F. (1975). The population effects of ecological sympatry on musk turtles on northern Florida. *Copeia* **1975**, 692-701.
Bohonak, A. J. and van der Linde, K. (2004). *RMA: Software for Reduced Major Axis regression, Java version*. Website: http://www.kimvdlinde.com/professional/rma.html.
Bulté, G., Irschick, D. J. and Blouin-Demers, G. (2008). The reproductive role hypothesis explains trophic morphology dimorphism in the northern map turtle. *Funct. Ecol.* **22**, 824-830.
Cleuren, J., Aerts, P. and De Vree, F. (1995). Bite and joint force analysis in *Caiman crocodilus*. *Belg. J. Zool.* **125**, 79-94.
Cochran, G. V. B. (1982). *A Primer of Orthopaedic Biomechanics*. New York: Churchill Livingstone.
Currey, J. D. (1980). Mechanical properties of mollusk shell. *Symp. Soc. Exp. Biol.* **34**, 75-87.
Curtis, N., Jones, M. E. H., Lappin, A. K., O'Higgins, P., Evans, S. E. and Fagan, M. J. (2010). Comparison between *in vivo* and theoretical bite performance: using multi-body modeling to predict muscle and bite forces in a reptile skull. *J. Biomech.* **43**, 2804-2809.
Dalrymple. G. H. (1977). Intraspecific variation in the cranial feeding mechanism of turtles of the genus *Trionyx* (Reptilia, Testudines, Trionychidae). *J. Herpetol.* **11**, 255-285.
Dalrymple, G. H. (1979). Packaging problems of head retraction in trionychid turtles. *Copeia* **1979**, 655-660.
Davis, J. L., Santana, S. E., Dumont, E. R. and Grosse, I. R. (2010). Predicting bite force in mammals: two-dimensional *versus* three-dimensional level models. *J. Exp. Biol.* **213**, 1844-1851.
De Vree, F. and Gans, C. (1984). Feeding in tetrapods. In *Biomechanics of Feeding in Vertebrates: Advances in Comparative and Environmental Physiology* (ed. V. L. Bels, M. Chardon and P. Vandewalle), pp. 93-118. Berlin: Springer Verlag.
Ellis, J. L., Thomason, J. J., Kebreab, E. and France, J. (2008). Calibration of estimating biting forces in domestic canids: comparison of post-mortem and *in vivo* measurements. *J. Anat.* **212**, 769-780.
Emerson, S. B. and Bramble, D. M. (1993). Scaling, allometry, and skull design. In *The Skull*, Vol. 3, *Functional and Evolutionary Mechanisms* (ed. J. Hanken and B. K. Hall), pp. 384-421. Chicago: University of Chicago Press.
Erickson, G. M., Lappin, A. K. and Vliet, K. A. (2003). The ontogeny of bite-force performance in American alligator (*Alligator mississippiensis*). *J. Zool. Lond.* **260**, 317-327.
Gans, C. and Bock, W. J. (1965). The functional significance of muscle architecture – a theoretical analysis. *Ergeb. Anat. Entwicklungsgesch.* **38**, 115-142.
Gans, C. and De Vree, F. (1987). Functional bases of fiber length and angulation in muscle. *J. Morphol.* **192**, 63-85.
Gans, C., De Vree, F. and Carrier, D. (1985). Usage pattern of the complex masticatory muscles in the shingleback lizard, *Trachydosaurus rugosus*: a model for muscle placement. *Am. J. Anat.* **173**, 219-240.
Grubich, J. (2005). Disparity between feeding performance and predicted muscle strength in the pharyngeal musculature of black drum, *Pogonias cromis* (Sciaenidae). *Environ. Biol. Fish.* **74**, 261-272.
Hernández, L. P. and Motta, P. J. (1997). Trophic consequences of differential performance: ontogeny of oral jaw-crushing performance in the sheepshead, *Archosargus probatocephalus* (Teleostei, Sparidae). *J. Zool. Lond.* **243**, 737-756.
Herrel, A. and Gibb, A. C. (2006). Ontogeny of performance in vertebrates. *Physiol. Biochem. Zool.* **79**, 1-6.
Herrel, A. and O'Reilly, J. C. (2006). Ontogenetic scaling of bite force in lizards and turtles. *Physiol. Biochem. Zool.* **79**, 31-42.
Herrel, A., Spithoven, L., Van Damme, R. and De Vree, F. (1999). Sexual dimorphism of head size in *Gallotia galloti*: testing the niche divergence hypothesis by functional analyses. *Funct. Ecol.* **13**, 289-297.
Herrel, A., Van Damme, R., Vanhooydonch, B. and De Vree, F. (2001). The implications of bite performance for diet in two species of lacertid lizards. *Can. J. Zool.* **79**, 662-670.
Herrel, A., O'Reilly, J. C. and Richmond, A. M. (2002). Evolution of bite performance in turtles. *J. Evol. Biol.* **15**, 1083-1094.
Herrel, A., Van Wassenbergh, S., Wouters, S., Adriaens, D. and Aerts, P. (2005). A functional morphological approach to the scaling of the feeding system in the African catfish, *Clarias gariepinus*. *J. Exp. Biol.* **208**, 2091-2102.
Herrel, A., De Smet, A., Aguirre, L. F. and Aerts, P. (2008). Morphological and mechanical determinants of bite force in bats: do muscles matter? *J. Exp. Biol.* **211**, 86-91.
Herrel, A., Podos, J., Vanhooydonck, B. and Hendry, A. P. (2009). Force-velocity trade-off in Darwin's finch jaw function: a biomechanical basis for ecological speciation? *Funct. Ecol.* **23**, 119-125.
Hill, A. V. (1950). The dimensions of animals and muscular dynamics. *Sci. Prog.* **38**, 209-230.
Huber, D. R. and Motta, P. J. (2004). Comparative analysis of methods for determining bite force in the spiny dogfish *Squalus acanthias*. *J. Exp. Zool.* **301A**, 26-37.
Huber, D. R., Eason, T. G., Hueter, R. E. and Motta, P. J. (2005). Analysis of the bite force and mechanical design of the feeding mechanism of the durophagous horn shark *Heterodontus francisci*. *J. Exp. Biol.* **208**, 3553-3571.

Huber, D. R., Weggelaar, C. L. and Motta, P. J. (2006). Scaling of bite force in the blacktip shark *Carcharhinus limbatus*. *Zoology* **109**, 109-119.
Huber, D. R., Dean, M. N. and Summers, A. P. (2008). Hard prey, soft jaws and the ontogeny of feeding mechanics in the spotted ratfish *Hydrolagus colliei*. *J. R. Soc. Interface* **5**, 941-952.
Kiltie, R. A. (1982). Bite force as a basis for niche differentiation between rain forest peccaries (*Tayassu tajacu* and *T. pecari*). *Biotropica* **14**, 188-195.
Kingsolver, J. G. and Huey, R. B. (2003). Introduction: the evolution of morphology, performance, and fitness. *Integr. Comp. Biol.* **43**, 361-366.
Kolmann, M. A. and Huber, D. R. (2009). Scaling of feeding biomechanics in the horn shark *Heterodontus francisci*: ontogenetic constraints on durophagy. *Zoology* **112**, 351-361.
MacArthur, R. H. and Pianka, E. R. (1966). On optimal use of a patchy environment. *Am. Nat.* **100**, 603-609.
Pfaller, J. B. (2009). Bite-force generation and feeding biomechanics in the loggerhead musk turtle, *Sternotherus minor*: implications for the ontogeny of performance. MSc thesis, Florida State University, Tallahassee, FL, USA.
Pfaller, J. B., Herrera, N. D., Gignac, P. M. and Erickson, G. M. (2010). Ontogenetic scaling of cranial morphology and bite-force generation in the loggerhead musk turtle. *J. Zool. Lond.* **280**, 280-289.
Powell, P. L., Roy, R. R., Kanim, P., Bello, M. A. and Edgerton, V. R. (1984). Predictability of skeletal muscle tension from architectural determinations in guinea pigs. *J. Appl. Physiol.* **57**, 1715-1721.
R Development Core Team (2008). A language and environment for statistical computing. R Foundation for Statistical Computing, Vienna. Available at: http://www.R-project.org.
Schmidt-Nielson, K. (1984). *Scaling: Why is Animal Size so Important?* Cambridge: Cambridge University Press.
Schumacher, G. (1973). The head muscles and hyolaryngeal skeleton of turtles and crocodilians. In *Biology of the Reptilia* (ed. C. Gans and T. S. Parsons), pp. 101-199. New York: Academic Press.
Schwenk, K. and Wagner, G. P. (2004). The relativism of constraints on phenotypic evolution. In *Phenotypic Integration* (ed. M. Pigliucci and K. Preston), pp. 390-408. Oxford: Oxford University Press.
Sinclair, A. G. and Alexander, R. M. (1987). Estimates of forces exerted by the jaw muscles of some reptiles. *J. Zool. Lond.* **213**, 107-115.
Sokal, R. R. and Rohlf, F. J. (2000). *Biometry*, 3rd edn. New York: W. H. Freeman.
Tinkle, D. W. (1958). The systematics and ecology of the *Sternothaerus carinatus* complex (Testudinata, Chelydridae). *Tulane Stud. Zool.* **6**, 1-56.
Van Daele, P. A. A. G., Herrel, A. and Adriaens, D. (2009). Biting performance in teeth-digging African mole-rats (*Fukomys*, Bathyergidae, Rodentia). *Physiol. Biochem. Zool.* **82**, 40-50.
Van der Meij, M. A. A. and Bout, R. G. (2004). Scaling of jaw muscle size and maximal bite force in finches. *J. Exp. Biol.* **207**, 2745-2753.
Van der Meij, M. A. A. and Bout, R. G. (2006). Seed husking time and maximal bite force in finches. *J. Exp. Biol.* **209**, 3329-3335.
Vermej, G. S. (1987). *Evolution and Escalation, an Ecological History of Life*. Princeton: Princeton University Press.
Verwaijen, D., Van Damme, R. and Herrel, A. (2002). Relationship between head size, bite force, prey handling efficiency and diet in two sympatric lacertid lizards. *Funct. Ecol.* **16**, 842-850.
Wainwright, P. C. (1987). Biomechanical limits to ecological performance: mollusk-crushing by the Caribbean hogfish, *Lachnolaimus maximus* (Labridae). *J. Zool. Lond.* **213**, 283-297.
Wyckmans, M., Van Wassenbergh, S., Adriaens, D., Van Damme, R. and Herrel, A. (2007). Size-related changes in cranial morphology affect diet in the catfish *Clariallabes longicauda*. *Biol. J. Linn. Soc.* **92**, 323-334.
Zappalorti, R. T. and Iverson, J. B. (2006). *Sternotherus minor* – loggerhead musk turtle. In *Biology and Conservation of Florida Turtles* (ed. P. Meylan), pp. 197-206. Chelonian Research Monographs No. 3. Lunenburg, MA: Chelonian Research Foundation.